The role of dispersive forces determining the energetics of adsorption in Ti zeolites

The role of dispersive forces determining the energetics of adsorption in Ti zeolites

Matteo Signorile,[1] Alessandro Damin,[*1] Francesca Bonino,[1] Valentina Crocellà,[1] Carlo Lamberti,[1,3,4] Silvia Bordiga[1,2]

Correspondence to: Alessandro Damin (E-mail: *alessandro.damin@unito.it*)

[1] *Matteo Signorile, Alessandro Damin, Francesca Bonino, Valentina Crocellà, Carlo Lamberti, Silvia Bordiga*
Department of Chemistry, NIS, and INSTM Reference Centre, Università di Torino, Via G. Quarello 15, I-10135 and Via P. Giuria 7, I-10125, Torino, Italy

[2] *Silvia Bordiga*
Department of Chemistry, University of Oslo, P.O. Box 1033, Oslo, Norway

[3] *Carlo Lamberti*
IRC "Smart Materials", Southern Federal University, Zorge street 5, 344090 Rostov-on-Don, Russia

[4] *Carlo Lamberti*
CrisDi, Università di Torino, Via P. Giuria 7, I-10125, Torino, Italy

ABSTRACT

Ti-zeolites are interesting materials because of their key role in partial oxidation reactions, as well as under a fundamental point of view being regarded as single site catalysts. Both experimental and computational approaches have been widely applied to the characterization of their active sites, reaching a level of knowledge unmatchable by most other important catalysts. However several question are still open, *e.g.* a proper energetic simulation of the adsorption process of simple molecules, fitting with the experimental outcomes, is missing. The present work wants to underline the role of dispersive forces in correctly determining the adsorption energies of H_2O and NH_3 in Ti chabazite: first dispersive contribution have been included through an ONIOM scheme, comparing the results from semiempirical Grimme scheme and fully *ab initio* MP2. Being the key contribution of dispersion proved, a fully periodic, Grimme dispersion inclusive approach has been applied, coming to results close to the experimental values.

1. Introduction

Ti-zeolites are a class of material covering a relevant niche in the field of heterogeneous catalysis. Characterized by the isomorphous substitution of the framework Si^{4+} with Ti^{4+},[1,2] they mainly find application in partial oxidation reactions in combination with hydrogen peroxide in aqueous solution. Since the largest part of these process are industrially performed in a liquid, aqueous medium, the interaction of these material with water is of outmost importance. Further, in most of the cases, ammonia is included in the reaction feeding as stabilizer for the hydrogen peroxide, in order to prevent its undesired decomposition: being a strong base, NH_3 can easily interact with the Ti sites, positively charged and so showing a Lewis acid character. The understanding of H_2O/NH_3 interaction with Ti-zeolites is determining in the understanding of their catalytic behavior, as testified by the numerous

studies devoted to their characterization.[3–11] Experimentally the energetic of interaction has been explored by calorimetric techniques,[3–5] while the coordination sphere and the structure of the Ti sites has been widely explored exploiting, vibrational, electronic spectroscopies and XAS.[11–15] Interesting reviews are available on the characterization of Ti-zeolites.[2,16–20] Some relevant improvements in the interpretation of the outcomes of experimental techniques arise from computational approaches: even with relatively simplified models and low cost computational methods, an accurate description of the vibrational and electronic fingerprints of Ti zeolites has been obtained.[10,15,21] Concerning the energetics of adsorption processes instead the results are more diverging from experimental results: according to Bolis and coworkers,[4,5] the measured heat of adsorption for a single NH_3 molecule per Ti site on Titanium Silicalite-1 falls in the range 60-70 $kJmol^{-1}$ depending on the measurement conditions. Previous computational studies, even if the structural features of the Ti center were properly simulated, were not able to give a right estimation of the interaction energies: cluster calculation on NH_3 monoadducts show BSSE corrected binding energies in the 30-40 $kJmol^{-1}$ range, heavily underestimating the entity of the measured interaction.[7,22,23] It is worth to stress that a cluster approach, being in the cited works of relatively small size, does not allow a correct description of the effect of the microporous structure of the zeolite, possibly stabilizing the adsorbate. However, also periodic simulation gave rise to very similar results.[6,9,24] A totally analogous situation was observed in the case of water adsorption. To the best of our knowledge, previous computational studies miss the inclusion/estimation of dispersive interactions, which has been shown to be fundamental in correctly describing both the structure of molecular crystals (e.g. 3D structure of proteins and DNA) and the adsorption phenomena on oxides, zeolites, etc.[25–31] Accounting for dispersion forces, the size of the considered system plays a relevant role: as recently commented by Wagner and Schreiner: *"For increasingly larger structures, the overall dispersion contribution grows rapidly and can amount to tens of kcalmol^{-1}"*.[32] This consideration is of great interest for the adsorption of small molecules in zeolites: the adsorbate, in fact, experiences the dispersions contribution from the whole framework, thus a large effect on the interaction energy is expected. From a quantum mechanical point of view, dispersion forces can be ascribed to the long-range electron correlations: a fully *ab initio* description of these interactions requires the use of correlated methods, such as Møller-Plesset perturbation theory or Coupled Cluster.[33–35] A possible, costless alternative to computationally demanding post Hartree-Fock methods is represented by the empirical estimation of dispersive forces introduced by Grimme:[26,36,37] the attractive forces among couples of atoms are evaluated through empirical C^6 coefficients, the reciprocal of the sixth-power of the atom-atom distance and are modulated by an appropriate damping function. In the present work the role of dispersive forces determining the adsorption energetics for ammonia and water in titanium chabazite (here adopted as a test case for Ti-zeolite) is explored: the advantage of such model is the lower size of the unit cell and (if fully exploited) the higher symmetry of the space group in comparison with the complex (but more relevant) Titanium Silicalite-1 (TS-1), but showing a very similar environment in the vicinity of the Ti site. It worth noticing that Ti-CHA was recently synthesized (Si/Ti =246) by the Lillerud group in Oslo[38] and that the spectroscopic responses (IR, UV-vis, Raman and Ti K-edge XANES) upon water adsorption of Ti(IV) sites in Ti-CHA are similar to those observed in TS-1.[11,15] In this work, the results from fully periodic DFT-D are compared with ones obtained through an ONIOM scheme, where dispersive interaction are included *ab initio* exploiting second order Møller-Plesset perturbation theory

(MP2). The outcomes of such analysis depict the key role of dispersions for a correct evaluation of energetic of adsorption processes in Ti-zeolites.

2. Computational Methods

2.1. Binding energy calculation

Binding energies for the adsorption processes were calculated according to Eq. 1

$$BE = E_a(A) + E_b(B) - E_{ab}(AB) \quad (1)$$

i.e. giving the energy which must be provided to dissociate the *AB* adduct, being *a* and *b* the basis sets for the *A* and *B* monomers respectively. The BE calculations were performed according to the process schematized in Eq. 2 and 3, *i.e.* considering two separate dissociations:

$$(AB^1)B^2 \rightarrow AB^1 + B^2 \quad (2)$$

$$AB^1 \rightarrow A + B^1 \quad (3)$$

where *A* is TiCHA and B^1 and B^2 are the first and the second ligand respectively. BSSE correction was adopted according to the literature,[39] exploiting the counterpoise method as shown in Eq. 4:

$$BE^c = BE - [E_a(A^{def}) - E_{ab}(A^{def}) + E_b(B^{def}) - E_{ab}(B^{def})] \quad (4)$$

In such equation, the "^{def}" superscript indicates that the geometry of the monomer after adsorption and relaxation is considered. Substituting Eq. 1 in Eq. 4 and conveniently rearranging the various terms it is possible to rewrite the latter as:

$$BE^c = [E_a(A) - E_a(A^{def}) + E_b(B) - E_b(B^{def})] + [E_{ab}(A^{def}) + E_{ab}(B^{def}) - E_{ab}(AB^{def})] \quad (5)$$

The second term is now split in two distinct contributions: the former takes in account the purely deformational contribution to the binding energies, *i.e.* the Deformation Energy DE; the latter represents the BSSE corrected formation energy for the adduct calculated starting from the already deformed monomers, indeed takes in account the energetic contributions to the BE^c due to the monomers interaction and can be labeled as BE^{defc}. On the basis of such consideration, Eq. 5 can be further rewritten as:

$$BE^c = DE + BE^{defc} \quad (6)$$

being

$$DE = E_a(A) - E_a(A^{def}) + E_b(B) - E_b(B^{def}) \quad (7)$$

$$BE^{defc} = E_{ab}(A^{def}) + E_{ab}(B^{def}) - E_{ab}(AB) \quad (8)$$

All these consideration are valid and were exploited for both periodic and ONIOM calculations.

2.2. Periodic computations

The periodic model of TiCHA was built up starting from the experimental geometry of purely siliceous chabazite:[40] a supercell (whose lattice parameters were derived from single cell ones according to Eq. 9) was obtained and geometry relaxation was performed.

$$a' = -a + b + c$$

$$b' = a - b + c \quad (9)$$

$$c' = a + b - c$$

Such cell contains 144 atoms and 48 equivalent Si sites. Consequently, a single silicon atom was substituted by a titanium one giving rise to a TiCHA model with Si/Ti ratio of 47 (corresponding to ~2.75 wt% of framework TiO_2, where typical TS-1 samples contain about 2 wt% TiO_2): the introduction of titanium causes the space group of the system to change from R $\bar{3}$ m to P1, *i.e.* the successive calculations were performed without taking advantage of the symmetry. The model was relaxed and exploited as starting point for the following adsorption simulation. Ammonia and water adsorption on the Ti site were studied. For both molecules, single and double coverage were considered: in the case of the adsorption of the second molecule, the relaxed geometry of the single adduct was used as starting point for the calculation. The periodic calculations were performed with the CRYSTAL14 code[41]: the B3LYP functional, combining the B3[42] hybrid exchange with the LYP[43] correlation functionals, was used. A double ζ quality basis set was used in the description of the periodic framework: 86-411G(d31) for Ti,[44] 88-31G(d1) for Si and 8-411G(d1) for O.[45] These basis sets are explicitly reported in Tables S1 of the Supporting Information. In the description of adsorbates, Ahlrichs TZV2P and TZV basis sets were exploited in the description of O/N and H respectively.[46] Thresholds for the mono- and bi-electronic integral (TOLINTEG) were set to {777714}. The shrinking factor parameters (SHRINK), determining the k-points sampling in the reciprocal space, were set to 2 2. The maximum order of shell multipoles in the long-range zone for the electron-electron Coulomb interaction (POLEORDR keyword) was chosen to be 6. The defaults values for the previously unreported computational parameters were used.[47] Dispersive forces were included in the calculation when required as implemented in the CRYSTAL code, *i.e.* accordingly to the Grimme two bodies (GD2) scheme.[47]

2.3. ONIOM computations

The ONIOM2 scheme as proposed by Morokuma et al. was applied in this work.[48] In this approach, the system is partitioned in two distinct layers: an inner part, containing the site of interest for the simulation (the so called model region), and the whole system (labeled as real model). For obvious reasons, the model region is treated with an higher level of theory (being so defined as High Model, HM), whereas for the real layer a less costly method (Low Real, LR) can be used. The ONIOM2 binding energy is then computed as reported in Eq. 10:

$$BE(ONIOM2) = BE(LR) - BE(LM) + BE(HM)$$
(10)

In order to properly compute the ONIOM2 energy, the contribution from the model region calculated at the low level method (Low Model) is included in Eq. 10. The presented ONIOM computations consist of single point energy calculations, adopting as LR the periodic TiCHA/TiCHA+NH_3 structures, as obtained from periodic calculations at the B3LYP level (see "Periodic computations" section for further details). Clusters of increasing size were considered as model region, ranging from 9 up to 55 real framework atoms (*i.e.* involving a fraction of the total atoms χ in the $0.06 < \chi < 0.38$ range). Their structure, in the form of NH_3 adducts, are schematized in Figure 1.

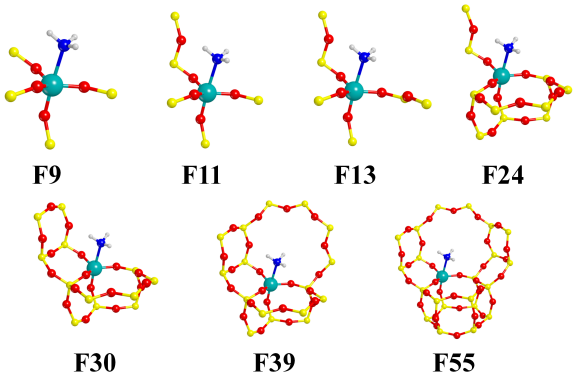

Figure 1. Ball and stick representation of the clusters used in the ONIOM calculations.

The dangling bonds on Si centers were saturated by hydrogen atoms, placed at a fixed distance of 1.45 Å. HM calculations on the model clusters were performed adopting B3LYP, B3LYP(D) and MP2 methods. The B3LYP, B3LYP(D) calculation on all the clusters were performed exploiting the Gaussian09 code,[49] as well as the MP2 on clusters from F9 to F24. For the three bulkier clusters (F30, F39, F55), the MP2 calculations were performed with NWChem in order to exploit the massive parallelization offered by the code.[50] In both cases, the MP2 calculation were limited to the valence electrons, freezing instead the core ones. A Dunning aug-cc-pVQZ basis set was chosen for anions (O and N), an Ahlrichs TZVP for cations (Ti and Si) and a Pople 6-311++G(2p,2d) for H atoms. All the G09/NWChem default computational parameters were used in the calculation. LM calculations on the model region were performed exploiting the CRYSTAL14 code, at the B3LYP level and with the same parameters used for the periodic calculations.

Table 1. B3LYP optimized cell volumes, Ti – O and Ti – N bond lengths for the CHA, TiCHA and TiCHA+NH_3 periodic models.

Model	Cell Volume ($Å^3$)	Ti – O_{ap} (Å)	Ti – O_{eq1} (Å)	Ti – O_{eq2} (Å)	Ti – O_{eq3} (Å)	<Ti – O> (Å)	Ti – N (Å)
CHA	3243	-	-	-	-	-	-
Ti-CHA	3263	1.803	1.799	1.794	1.809	1.801	-
Ti-CHA+NH_3	3259	1.844	1.821	1.809	1.838	1.828	2.359

3. Results and Discussion

3.1. Periodic construction of the starting TiCHA(+NH_3) model

As starting model for the following calculations, TiCHA and TiCHA+NH_3 periodic models were optimized without including dispersive forces. The optimized cell volume and the distances among the Ti center and its O/N first neighbors are reported in Table 1. The full set of relaxed cell parameters is given in Table S2. The introduction of the Ti atom in the siliceous framework of CHA leads to a slight expansion of the cell as demonstrated by the increase of the cell parameters and, consequently, of the cell volume due to an average Ti–O distance in the 1.79-1.81 Å range[4,5,13,14,51] much larger than the typical average Si–O distance in zeolites: 1.60 Å.[40,52] Conversely, the cell angles are only slightly modified. The entity of the expansion, about 0.6%, is perfectly matching the experimental evidences obtained on TS-1, where diffraction experiments show an increase of the cell volume of 0.8% at comparable Ti contents.[53] By comparison, the geometry relaxation of a TiCHA model based on a single CHA (Si/Ti = 11)[9] cell leaded to an unrealistic cell volume expansion of about 3% (see Table S3 of the Supplementary Information). Introducing the NH_3 adsorbate a negligible reduction of the cell size is observed, whereas in the case of the single cell model a reduction of -0.4% was computed. The reported data confirmed the good choice of a supercell model, as it allows to properly describe the system thanks to its realistic Ti loading. Looking closer at the Ti coordination sphere more significant deformation effects are observed upon ammonia adsorption. The unperturbed Ti site exhibits an almost perfectly tetrahedral local symmetry and an average Ti – O distance in good agreement with the experimental distance of 1.79 Å obtained on dehydrated TS-1 by EXAFS.[4,5,13,14,51] After the NH_3 adsorption, the local geometry of the Ti site is significantly altered: all the Ti – O distances are enlarged (as experimentally observed by EXAFS) and the local T_d symmetry is broken. In particular the distance between Ti and the O in apical position with respect to the ligand NH_3 is the most affected, whereas the equatorial oxygen atoms react in a heterogeneous way to the occurred adsorption. Considering the average Ti – O distance upon adsorption, this is slightly underestimated in comparison with the experimental values (1.88 Å for EXAFS, measurements with 2 adsorbed NH_3 molecules per Ti atom), however the correct trend (i.e. expansion) is observed as already commented. [5,16] Clusters used in the ONIOM calculation were extracted from these structures: the seven models whose structures are depicted in Figure 1. The calculated BE^c are reported in Table 2 and graphically outlined in Figure 2.

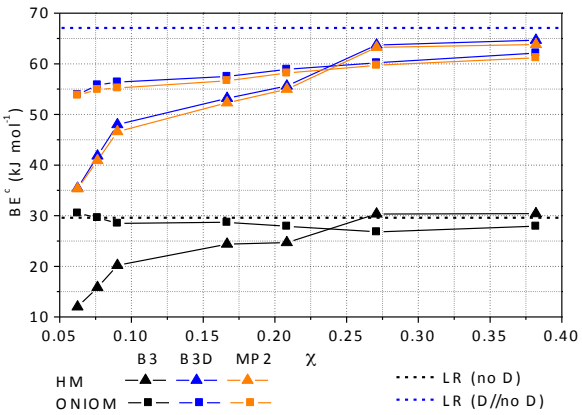

Figure 2. BE^c *vs* fraction of real atoms included in the model region with respect to the low real model (χ). See Table also 2.

Table 2. HM and ONIOM BSSE corrected Binding Energies (BE^c) for the seven model cluster at different computational levels. All the value are reported in $kJmol^{-1}$. χ represent the fraction of unit cell atoms included in the cluster. Reported values are plotted in Figure 2 as a function of the fraction of unit cell atoms included in the cluster χ.

Model	F9	F11	F13	F24	F30	F39	F55	LR
χ	0.06	0.08	0.09	0.17	0.21	0.27	0.38	1.00
$B3LYP_{CRY}$								
BE^C (LR)	-	-	-	-	-	-	-	29.6
BE^C (LM)	11.1	15.7	21.3	25.2	26.4	33.1	32.1	-
$B3LYP(D)_{CRY}$ //$B3LYP_{CRY}$								
BE^C (LR)	-	-	-	-	-	-	-	67.1
$B3LYP//B3LYP_{CRY}$								
BE^C (HM)	12.0	15.7	20.2	24.3	24.7	30.3	30.4	-
BE^C (ONIOM)	30.5	29.6	28.5	28.7	27.9	26.8	27.9	-
$B3LYP(D)//B3LYP_{CRY}$								
BE^C (HM)	35.4	41.9	48.0	53.2	55.6	63.7	64.7	-
BE^C (ONIOM)	53.9	55.8	56.4	57.5	58.9	60.2	62.1	-
$MP2//B3LYP_{CRY}$								
BE^C (HM)	35.3	40.9	46.9	52.3	55.0	63.2	63.8	-
BE^C (ONIOM)	53.8	54.9	55.2	56.7	58.2	59.7	61.2	-

Concerning the low model, the computed BSSE corrected binding energy rapidly converges to the value calculated for the full, low real periodic model: the larger increases of the BE^c at the first cluster enlargements can be ascribed to a proper inclusion of the major electrostatic contributions, whereas this growth is reduced as farer atoms are added to the model region. Unexpectedly the last two clusters exhibit a considerably larger BE^c in comparison to the previous ones; furthermore, a small reduction in the BE^c is observed moving from cluster F39 to the much bigger F55. Despite this oscillating behavior (no more than 6 $kJmol^{-1}$), possibly due to bad compensation among the three layers, a reasonable overall convergence is achieved. This interpretation is confirmed by looking at the energetic of the $B3LYP//B3LYP_{CRY}$ high models: exploiting the higher precision proper of a molecular calculation the BE^c show a smoother, monotonic trend also in the bigger clusters. Also in this case, a fast convergence to the BE^c(LR) value is observed. As a consequence of the larger value of BE^c(LM) compared to BE^c(LR) the ONIOM binding energies for the bigger clusters are smaller than the respective for the HM; however it is

worth to underline that also in these cases the energy difference between BE^c(HM) and BE^c(ONIOM) is below 3 kJmol^{-1}, a significantly small value allowing a proper comparison with experimental values. All the results achieved without including dispersive forces are in good agreement with the previous computational literature,[7,9] so largely underestimating the TiCHA-NH_3 interaction energy. The situation totally changes as dispersions are considered, both empirically (B3LYP(D)//$B3LYP_{CRY}$) or *ab initio* (MP2//$B3LYP_{CRY}$): also for the smaller cluster, the binding energy is significantly increased, rapidly converging to the $B3LYP(D)_{CRY}$//$B3LYP_{CRY}$ BE^c(LR) reference value. The difference between the BE^c(HM) computed at B3LYP(D)//$B3LYP_{CRY}$ and at B3LYP//$B3LYP_{CRY}$ represents the purely dispersive contribution to the Binding Energy: being 23.4 kJmol^{-1} for the smaller cluster (F9), it reaches the value of 34.3 kJmol^{-1} for the bigger one (F55), showing an increase of 10.9 kJmol^{-1}. By comparison, the dispersive contribution calculated on the BE^c(LR) is 37.5 kJmol^{-1}: such result demonstrates that the F55 fragment is sufficiently big to take in account the 91% of the total dispersive contribution, being so an effective model in describing the NH_3 adsorption on TiCHA even with a cluster approach. A quite similar result is achieved by including dispersive forces *ab initio* through the correlated MP2 method: the computed binding energies are of the same magnitude of B3LYP(D)//$B3LYP_{CRY}$, being in average 0.5 kJmol^{-1} lower. To verify the accuracy of the calculation, a Complete Basis Set extrapolation on the BE^c(HM) for the F9 model was performed: comparing the values obtained with the aug-cc-pVQZ and extrapolated at CBS, these are really similar, testifying the goodness of the adopted approach (see Figure S1 and Table S4 for details). On this model, also CCSD and CCSD(T) calculation and CBS extrapolation were performed: the former leaded to results in line with the MP2 ones, while the latter showed an energy gain of about 3 kJmol^{-1}. However MP2 can be regarded as a reasonable benchmark method in this study, also considering the almost unaffordable cost of coupled cluster calculations. In order to better characterize the contributions to the BE^c, the Deformation Energies (DE) and the Binding Energies for the already deformed monomers (BE^{defc}) were computed as reported in Table 3.

Table 3. Deformation Energies (DE) and the Binding Energies for the already deformed monomers (BE^{defc}) for the seven model cluster at different computational levels. All the value are reported in kJmol^{-1}.

Model	χ	B3LYP//$B3LYP_{CRY}$		B3LYP(D)//$B3LYP_{CRY}$		MP2//$B3LYP_{CRY}$	
		DE	BE^{defc}	DE	BE^{defc}	DE	BE^{defc}
F9	0.06	-44.6	56.6	-43.7	79.1	-42.7	78.0
F11	0.08	-42.6	58.2	-41.6	83.4	-40.6	81.5
F13	0.09	-40.5	60.7	-39.0	87.0	-38.2	85.0
F24	0.17	-40.7	65.0	-39.2	92.4	-37.8	90.1
F30	0.21	-41.5	66.2	-39.8	95.4	-38.1	93.0
F39	0.27	-40.5	70.8	-39.0	102.7	-36.6	99.8
F55	0.38	-40.9	71.3	-39.1	103.7	-36.9	100.6

It is possible to observe that the DE are pretty similar among the different methods, as well as considering the different cluster sizes. Conversely the BE^{defc} are approximately 40% larger as dispersions are included (both empirically and *ab initio*) and increases as the cluster size increase. This result suggest the importance of dispersive forces in simulating correctly the TiCHA-NH_3 interaction: the bonding and non-bonding electrostatic contributions determines about the 60% of the final binding energy and, since

the energy contribution of the deformation is in first approximation constant, the missing fraction of the BE^c is univocally ascribable to dispersive forces.

3.2. Fully periodic approach

Being the role of dispersive forces demonstrated, a fully periodic, dispersion inclusive (through the Grimme GD2 scheme) approach to the complexation of TiCHA with ammonia and water was exploited: the dispersion contributions were directly included in the geometry relaxation. The obtained relaxed structures are sketched in Figure 3. The optimized geometries cell volumes for the H_2O and NH_3 mono- and bi-adducts with TiCHA are shown in Table 4 together with the Ti – O and Ti – Ligand distances.

Table 4. B3LYP(D) optimized cell volumes, Ti – O and Ti – L (where L is the N/O atom of the adsorbate) bond lengths for the CHA, TiCHA and TiCHA+H_2O/NH_3 mono- and bi-adducts periodic models.

Model	Cell Volume (Å^3)	Ti – O_{ap} (Å)	Ti – O_{eq1} (Å)	Ti – O_{eq2} (Å)	Ti – O_{eq3} (Å)	<Ti – O> (Å)	Ti – L^1 (Å)	Ti – L^2 (Å)
CHA	3180	-	-	-	-	-	-	-
Ti-CHA	3204	1.809	1.781	1.802	1.806	1.799	-	-
Ti-CHA + H_2O^1	3208	1.832	1.808	1.818	1.824	1.820	2.379	-
+ H_2O^2	3201	1.882	1.831	1.840	1.848	1.850	2.263	2.330
Ti-CHA + NH_3^1	3202	1.840	1.802	1.834	1.839	1.829	2.328	-
+ NH_3^2	3183	1.868	1.853	1.855	1.868	1.861	2.343	2.307

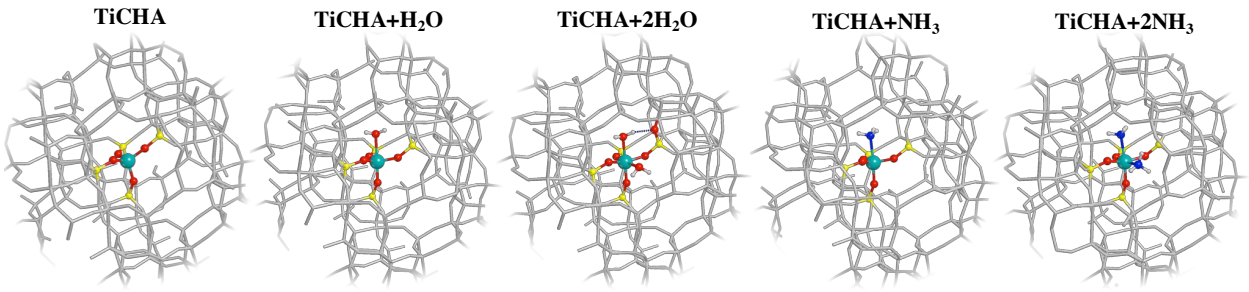

Figure 3. Graphical representation of the periodic models after relaxation.

The detailed relaxed cell parameters are given in Table S5. The data for the bare CHA and TiCHA are reported as well. Also including the dispersive interactions in the geometry relaxation, the expansion due to the Ti insertion in the CHA framework is even more close to the experimental one, reaching the 0.8%. Furthermore, the reliability of the supercell model allows to perform the adsorption simulation with negligible geometrical deformation in the zeolitic framework. Only in the case of double ammonia adsorption the cell volume is significantly changing, being similar to the one of the bare CHA. Moving the local structure of the Ti center, the average Ti – O distance upon adsorption is increased: in the case of NH_3 the introduction of a second adsorbed molecule brings closer to the expected experimental value of 1.88 Å.[4,5] Conversely with water the average <Ti – O> value for a single adsorption is matching experimental one (1.82 Å), whereas is slightly overestimated following the second adsorption.[5,16]

However the general description of the Ti-site local environment is quite reliable and phenomenologically sound. Considering the Ti – L distances, fairly different behavior are observed for water and ammonia: in the case of H_2O, as the second molecule is adsorbed the Ti – L^1 distance is reduced, being smaller than the Ti – L^2 one; conversely for NH_3 a slightly increase of Ti – L^1 is observed upon the second adsorption, whereas the Ti – L^2 is the shorter. The shortening of Ti – L^1 distance for water is explained by the formation of an hydrogen bond among the H_2O molecule and a Ti third neighbor oxygen framework atom thanks to the framework deformation induced by the second adsorption. Becoming the water oxygen more polarized, it is able to interact more strongly with the Ti center so showing the shorter Ti – OH_2 distance. In the case of ammonia, the second adsorption induces a sudden change in the system, as already inferred by looking at the unexpected volume reduction. The addition of a second NH_3 molecules is probably able to significantly detach the Ti from the framework, as also testified by the considerable increase in the average Ti – O distances. The framework responses to this "detachment" with a partial recovery of its originally, siliceous structure as the volume contraction to values proper of the CHA model suggests. For what concerns the energetics of the adsorption processes, the BE^c values reported in Table 5 are in good agreement with the experimental data.

Table 5. B3LYP(D) BSSE corrected Binding Energies (BE^c), Deformation Energies (DE) and the Binding Energies for the already deformed monomers (BE^{defc}) for the TiCHA and TiCHA+H_2O/NH_3 mono- and bi-adducts periodic models. All the value are reported in kJmol^{-1}.

Model	BE^c	DE	BE^{defc}
Ti-CHA + H_2O^1	50.8	-35.8	86.7
+ H_2O^2	45.7	-32.2	78.0
Ti-CHA + NH_3^1	69.6	-48.3	118.0
+ NH_3^2	52.2	-62.4	114.6

Referring to the data of Bolis and coworkers on NH_3 adsorption,[4,5] an heat of adsorption of 66 kJmol^{-1} is expected for a single adsorption whereas a slightly lower 55 kJmol^{-1} is ascribed to the second one: the computed binding energies, 69.6 kJmol^{-1} and 52.2 kJmol^{-1} respectively, are for the first time approaching the experimental values. Similarly, the literature value expected for water adsorption of about 50 kJmol^{-1} is correctly reproduced.[3] It is important to note that a proper comparison should be performed with calculated enthalpies, so requiring a full frequency calculation in order to estimate the zero point energy, the thermal energy and the *pV* contributions: being these computations really costly on the chosen periodic system, they have not been considered in the present work. However, at least in an approximated ground, the agreement with experimental data is really promising and demonstrates the reliability of the TiCHA model in the simulation of adsorption on Ti zeolites. Considering the DE and BE^{defc}, as already commented in relation to geometrical parameters, the trends observed for water and ammonia adsorption are substantially different. The H_2O shows a reduction of both DE and BE^{defc} upon the introduction of the second molecule, consistently with a pure adsorption process: the first molecule causes the deformation of the framework and strongly interacts with the Ti, whereas the following insertion of the second one requires a lower deformation energy but also give rise to a weaker interaction. Consequently, the BE^c for the second adsorption is lower than the first as expected. Conversely, in the case of NH_3, the second adsorption requires a much larger DE to move the Ti atom in

its new “quasi-extraframework” position, being the whole zeolite framework seriously involved in a partial reconversion in a purely siliceous like structure. However the new ligand is fundamental in stabilizing the new local structure of the Ti, as testified by the slight reduction of the BE^{defc} with respect to the first adsorption process.

4. Conclusions

The present work demonstrated the importance of dispersive forces in the correct evaluation of adsorption energetics of water and ammonia on a model Ti-zeolite (TiCHA). Independently from the method chosen for their evaluation (empirical Grimme scheme or *ab initio* MP2), the inclusion of dispersions in the ONIOM approach give rise to an increase of about 50% on the final binding energy, so having a comparable weight compared to the purely electrostatic and charge transfer contributions. Strong of this result, water and ammonia adsorption with single and double coverage was performed with a fully periodic approach including empirically dispersion forces. The outcomes interestingly underlined the different behavior of the two molecules, with the water being simply adsorbed, whereas a reactivity toward the framework Ti is inferred for ammonia (at least at the highest coverage). These findings are really relevant since can represent the starting point for de-titanation processes possibly occurring at the reaction condition, arousing a change in the Ti sites speciation and determining an irreversible modification to the overall catalytic activity of the Ti-zeolite. It is finally worth comparing our calculation data with the recent experimental work of Gallo et al.,[11] who used valence to core X-ray emission spectroscopy (vtc-XES)[54–56] to investigate TS-1 before and after interaction with H_2O and NH_3. In that work authors found that, for both adsorbates, the experimental vtc-XES maps were better reproduced by the theoretical maps computed on the basis of a cluster containing only one ligand molecule rather than two. This finding is in apparent contradiction with the computational results reported here, where the addition of a second ligand has BE^c values comparable to that of the first absorbed molecule (see Table 5), making the insertion of a second ligand (H_2O or NH_3) energetically favored. The disagreement between these two studies may be cured by considering the three aspects. (i) The high photon flux emitted by the two ondulators of the ID26 beamline of the ESRF may cause a photon-induced desorption of the second ligand. (ii) The theoretical vtc-XES maps computed by Gallo et al.[11] were obtained on a large cluster, but without taking into account the effect of the dispersive interactions as done here. (iii) While the Ti-CHA framework exhibits only one crystallographic independent T sites, TS-1 (MFI topology) has 12. This means that all Ti atoms inserted in the CHA framework will have the same local environment, having room to host up to two ligands. Instead, some of the T sites of the MFI framework, found to be favorable for Ti insertion by neutron diffraction data,[57] are more sterically hindered by surroundings because of the different channel topology. This is the case of sites T7 and T11, whereas T6 site, sitting at the channels intersection of the MFI structure, could coordinate up to two ligands (H_2O or NH_3).

Acknowledgments

This work was performed on the Abel Cluster, owned by the University of Oslo and the Norwegian metacenter for High Performance Computing (NOTUR), in the framework of the N9381K NOTUR grant. The authors acknowledge: the Theoretical Chemistry Group, Università di Torino for providing the

CRYSTAL14 code and for their precious suggestions; Dr. F. Schmidt (Evonik Industries AG), Dr. H. Morell (Evonik Industries AG) and prof. G. Ricchiardi (Università di Torino) for the fruitful discussion. CL thank the Russian Ministry of Education and Science for the support (megagrant no. 14.Y26.31.0001).

Keywords: Zeolite, DFT, adsorption, dispersive-interaction, Ti-silicate

Additional Supporting Information may be found in the online version of this article.

References and Notes

[1] B. Notari, G. Perego, M. Taramasso, *Preparation of Porous Crystalline Synthetic Material Comprised of Silicon and Titanium Oxides*, **1983**, US 06/393,379.

[2] B. Notari, in *Adv. Catal.* (Eds.: D.D. Eley, W.O. Haag, B. Gates), Elsevier Academic Press Inc, San Diego, **1996**, pp. 253–334.

[3] T. Blasco, M. Camblor, A. Corma, P. Esteve, J. M. Guil, A. Martı, S. Valencia, A. Martinez, J. Perdigon-Melon, *J. Phys. Chem. B* **1998**, *102*, 75–88.

[4] V. Bolis, S. Bordiga, C. Lamberti, A. Zecchina, A. Carati, F. Rivetti, G. Spanò, G. Petrini, *Langmuir* **1999**, *15*, 5753–5764.

[5] V. Bolis, S. Bordiga, C. Lamberti, A. Zecchina, A. Carati, F. Rivetti, G. Petrini, G. Spanò, *Microporous Mesoporous Mater.* **1999**, *30*, 67–76.

[6] C. M. Zicovich-Wilson, R. Dovesi, A. Corma, *J. Phys. Chem. B* **1999**, *103*, 988–994.

[7] A. Damin, S. Bordiga, A. Zecchina, C. Lamberti, *J. Chem. Phys.* **2002**, *117*, 226–237.

[8] S. Bordiga, A. Damin, F. Bonino, G. Ricchiardi, A. Zecchina, R. Tagliapietra, C. Lamberti, *Phys. Chem. Chem. Phys.* **2003**, *5*, 4390–4393.

[9] A. Damin, S. Bordiga, A. Zecchina, K. Doll, C. Lamberti, *J. Chem. Phys.* **2003**, *118*, 10183–10194.

[10] E. Fois, A. Gamba, G. Tabacchi, *ChemPhysChem* **2008**, *9*, 538–543.

[11] E. Gallo, F. Bonino, J. C. Swarbrick, T. Petrenko, A. Piovano, S. Bordiga, D. Gianolio, E. Groppo, F. Neese, C. Lamberti, et al., *ChemPhysChem* **2013**, *14*, 79–83.

[12] D. Scarano, A. Zecchina, S. Bordiga, F. Geobaldo, G. Spoto, G. Petrini, G. Leofanti, M. Padovan, G. Tozzola, *J. Chem. Soc. Faraday Trans.* **1993**, *89*, 4123.

[13] S. Bordiga, F. Boscherini, S. Coluccia, F. Genonic, C. Lamberti, G. Leofanti, L. Marchese, G. Petrini, G. Vlaic, A. Zecchina, *Catal. Letters* **1994**, *26*, 195–208.

[14] S. Bordiga, S. Coluccia, C. Lamberti, L. Marchese, A. Zecchina, F. Boscherini, F. Buffa, F. Genoni, G. Leofanti, *J. Phys. Chem.* **1994**, *98*, 4125–4132.

[15] G. Ricchiardi, A. Damin, S. Bordiga, C. Lamberti, G. Spano, F. Rivetti, A. Zecchina, G. Spanò, F. Rivetti, A. Zecchina, *J. Am. Chem. Soc.* **2001**, *123*, 11409–11419.

[16] S. Bordiga, F. Bonino, A. Damin, C. Lamberti, *Phys. Chem. Chem. Phys.* **2007**, *9*, 4854–4878.

[17] P. Ratnasamy, D. Srinivas, H. Knözinger, **2004**, *48*, 1–169.

[18] S. Bordiga, E. Groppo, G. Agostini, J. A. Van Bokhoven, C. Lamberti, **2013**, *113*, 1736–1850.

[19] L. Nemeth, S. R. Bare, **2014**, *57*, 1–97.

[20] J. A. van Bokhoven, C. Lamberti, *Coord. Chem. Rev.* **2014**, *277*, 275–290.

[21] S. Bordiga, A. Damin, F. Bonino, A. Zecchina, G. Spanò, F. Rivetti, V. Bolis, C. Prestipino, C. Lamberti, *J. Phys. Chem. B* **2002**, *106*, 9892–9905.

[22] P. E. Sinclair, G. Sankar, C. R. A. Catlow, J. M. Thomas, T. Maschmeyer, *J. Phys. Chem. B* **1997**, *101*, 4232–4237.

[23] H. Munakata, Y. Oumi, A. Miyamoto, *J. Phys. Chem. B* **2001**, *105*, 3493–3501.

[24] G. Ricchiardi, A. de Man, J. Sauer, *Phys. Chem. Chem. Phys.* **2000**, *2*, 2195–2204.

[25] P. Ugliengo, A. Damin, *Chem. Phys. Lett.* **2002**, *366*, 683–690.

[26] S. Grimme, *J. Comput. Chem.* **2004**, *25*, 1463–1473.

[27] J. Antony, S. Grimme, *Phys. Chem. Chem. Phys.* **2006**, *8*, 5287–5293.

[28] T. Kerber, M. Sierka, J. Sauer, *J. Comput. Chem.* **2008**, *29*, 2088–2097.

[29] B. Civalleri, C. M. Zicovich-Wilson, L. Valenzano, P. Ugliengo, *CrystEngComm* **2008**, *42*, 4–6.

[30] S. Tosoni, J. Sauer, *Phys. Chem. Chem. Phys.* **2010**, *12*, 14330–40.

[31] M. Delle Piane, M. Corno, R. Orlando, R. Dovesi, P. Ugliengo, *Chem. Sci.* **2016**, *7*, 1496–1507.

[32] J. P. Wagner, P. R. Schreiner, *Angew. Chemie - Int. Ed.* **2015**, *54*, 12274–12296.

[33] S. Kristyán, P. Pulay, *Chem. Phys. Lett.* **1994**, *229*, 175–180.

[34] P. Hobza, J. Sponer, T. Reschel, *J. Comput. Chem.* **1995**, *16*, 1315–1325.

[35] M. J. Allen, D. J. Tozer, *J. Chem. Phys.* **2002**, *117*, 11113–11120.

[36] S. Grimme, *J. Comput. Chem.* **2006**, *27*, 1787–1799.

[37] S. Grimme, J. Antony, S. Ehrlich, H. Krieg, *J. Chem. Phys.* **2010**, *132*, 154104 1–19.

[38] E. A. Eilertsen, S. Bordiga, C. Lamberti, A. Damin, F. Bonino, B. Arstad, S. Svelle, U. Olsbye, K. P.

Lillerud, *ChemCatChem* **2011**, *3*, 1869–1871.

[39] G. Lendvay, I. Mayer, *Chem. Phys. Lett.* **1998**, *297*, 365–373.

[40] M.-J. Díaz-Cabañas, P. A. Barrett, *Chem. Commun.* **1998**, 1881–1882.

[41] R. Dovesi, R. Orlando, A. Erba, C. M. Zicovich-Wilson, B. Civalleri, S. Casassa, L. Maschio, M. Ferrabone, M. De La Pierre, P. D'Arco, et al., *Int. J. Quantum Chem.* **2014**, *114*, 1287–1317.

[42] A. D. Becke, *J. Chem. Phys.* **1993**, *98*, 1372.

[43] C. Lee, W. Yang, R. G. Parr, *Phys. Rev. B* **1988**, *37*, 785–789.

[44] http://www.crystal.unito.it/Basis_Sets/titanium.html#Ti_86-411%28d31%29G_darco_unpub, "http://www.crystal.unito.it/Basis_Sets/titanium.html#Ti_86-411%28d31%29G_darco_unpub," **n.d.**

[45] R. Nada, J. B. Nicholas, M. I. McCarthy, A. C. Hess, *Int. J. Quantum Chem.* **1996**, *60*, 809–820.

[46] A. Schäfer, C. Huber, R. Ahlrichs, *J. Chem. Phys.* **1994**, *100*, 5829.

[47] Dovesi R., V. R. Saunders, C. Roetti, R. Orlando, C. M. Zicovich-Wilson, F. Pascale, B. Civalleri, K. Doll, N. M. Harrison, I. J. Bush, et al., *http://www.crystal.unito.it/Manuals/crystal14.pdf,* **2014**.

[48] S. Dapprich, I. Komáromi, K. S. Byun, K. Morokuma, M. J. Frisch, *J. Mol. Struct. THEOCHEM* **1999**, *461-462*, 1–21.

[49] M. J. Frisch, G. W. Trucks, H. B. Schlegel, G. E. Scuseria, M. A. Robb, J. R. Cheeseman, G. Scalmani, V. Barone, B. Mennucci, G. A. Petersson, et al., *Gaussian 09 Revis. D.03,* **2009**.

[50] M. Valiev, E. J. Bylaska, N. Govind, K. Kowalski, T. P. Straatsma, H. J. J. Van Dam, D. Wang, J. Nieplocha, E. Apra, T. L. Windus, et al., *Comput. Phys. Commun.* **2010**, *181*, 1477–1489.

[51] D. Gleeson, G. Sankar, C. Richard A. Catlow, J. Meurig Thomas, G. Spanó, S. Bordiga, A. Zecchina, C. Lamberti, *Phys. Chem. Chem. Phys.* **2000**, *2*, 4812–4817.

[52] G. Artioli, C. Lamberti, G. L. Marra, *Acta Crystallogr. Sect. B Struct. Sci.* **2000**, *56*, 2–10.

[53] C. Lamberti, S. Bordiga, A. Zecchina, A. Carati, N. N. Fitch, G. Artioli, G. Petrini, M. Salvalaggio, G. L. L. Marra, *J. Catal.* **1999**, *183*, 222–231.

[54] P. Glatzel, U. Bergmann, *Coord. Chem. Rev.* **2005**, *249*, 65–95.

[55] J. Singh, C. Lamberti, J. A. van Bokhoven, *Chem. Soc. Rev.* **2010**, *39*, 4754–4766.

[56] E. Gallo, C. Lamberti, P. Glatzel, *Phys. Chem. Chem. Phys.* **2011**, *13*, 19409.

[57] C. Lamberti, S. Bordiga, A. Zecchina, G. Artioli, G. Marra, G. Spanò, *J. Am. Chem. Soc.* **2001**, *123*,

2204–2212.

GRAPHICAL ABSTRACT

Matteo Signorile, Alessandro Damin, Francesca Bonino, Valentina Crocellà, Carlo Lamberti, Silvia Bordiga

The role of dispersive forces determining the energetics of adsorption in Ti zeolites

Dispersive interactions allows the proper description of adsorption energetic for water and ammonia, whereas a purely electronic description largely underestimates the interaction energy.

$$E = E_{el} + E_{disp}$$

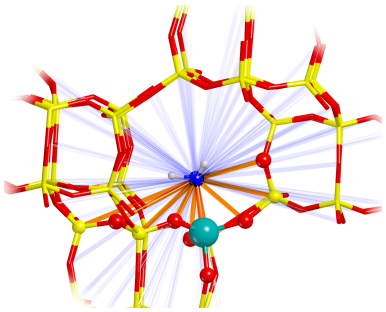

Supporting Information for

The role of dispersive forces determining the energetics of adsorption in Ti zeolites

Matteo Signorile,[1] Alessandro Damin,[*1] Francesca Bonino,[1] Valentina Crocellà,[1] Carlo Lamberti,[1,3,4] Silvia Bordiga[1,2]

Correspondence to: Alessandro Damin (E-mail: *alessandro.damin@unito.it*)

[1] *Matteo Signorile, Alessandro Damin, Francesca Bonino, Valentina Crocellà, Carlo Lamberti, Silvia Bordiga Department of Chemistry, NIS, and INSTM Reference Centre, Università di Torino, Via G. Quarello 15, I-10135 and Via P. Giuria 7, I-10125, Torino, Italy*

[2] *Silvia Bordiga*
Department of Chemistry, University of Oslo, P.O. Box 1033, Oslo, Norway

[3] *Carlo Lamberti*
IRC "Smart Materials", Southern Federal University, Zorge street 5, 344090 Rostov-on-Don, Russia

[4] *Carlo Lamberti*
CrisDi, Università di Torino, Via P. Giuria 7, I-10125, Torino, Italy

In Table S1 the basis set exploited in the TiCHA periodic calculation (in the CRYSTAL format) are reported.

Table S1. Ti, Si and O basis sets exploited in the TiCHA periodic calculation.

Ti: 86-411G(d31)	**Si: 88-31G(d1)**	**O: 8-411G(d1)**
22 7	14 5	8 5
0 0 8 2. 1.	0 0 8 2.0 1.0	0 0 8 2.0 1.0
225338.0 0.000228	149866.0 0.0001215	8966.29 0.001
32315.0 0.001929	22080.6 0.0009770	1240.17 0.0091
6883.61 0.011100	4817.5 0.0055181	252.114 0.0513
1802.14 0.05	1273.5 0.0252000	70.359 0.1702
543.063 0.17010	385.11 0.0926563	23.9025 0.3662
187.549 0.369	128.429 0.2608729	9.2075 0.3859
73.2133 0.4033	45.4475 0.4637538	3.9847 0.1471
30.3718 0.1445	16.2589 0.2952000	1.2266 0.0695
0 1 6 8. 1.	0 1 8 8.0 1.0	0 1 4 8.0 1.0
554.042 -0.0059 0.0085	881.111 -0.0003 0.0006809	44.9344 -0.0098 0.0107
132.525 -0.0683 0.0603	205.84 -0.0050 0.0059446	10.3978 -0.0893 0.067
43.6801 -0.1245 0.2124	64.8552 -0.0368 0.0312000	3.297 -0.0373 0.21
17.2243 0.2532 0.3902	23.9 -0.1079 0.1084000	1.234 0.373 0.3542
7.2248 0.6261 0.4097	10.001 0.0134 0.2378000	0 1 1 0.0 1.0
2.4117 0.282 0.2181	4.4722 0.3675 0.3560066	0.4536 1.0 1.0
0 1 4 8. 1.	2.034 0.5685 0.3410000	0 1 1 0.0 1.0
24.4975 0.0175 -0.0207	0.9079 0.2065 0.1326000	0.181 1.0 1.0
11.4772 -0.2277 -0.0653	0 1 3 4.0 1.0	0 3 1 0.0 1.0
4.4653 -0.7946 0.1919	2.6668 -0.0491 0.0465000	0.6 1.0
1.8904 1.0107 1.3778	1.0780 -0.1167 -0.1005000	
0 1 1 2. 1.	0.3682 0.2300 -1.0329000	
0.8099 1.0 1.0	0 1 1 0.0 1.0	
0 1 1 0. 1.	0.193 1.0 1.0	
0.3242 1.0 1.0	0 3 1 0. 1.	
0 3 3 2. 1.	0.610 1.0	
7.6781 0.1127		
1.8117 0.3927		
0.463 0.5206		
0 3 1 0. 1.		
0.23 1.0		

In Table S2 the full set of relaxed cell parameters for the CHA, TiCHA and TiCHA+NH_3 periodic models obtained at the B3LYP level are reported.

Table S2. B3LYP optimized cell parameters for the CHA, TiCHA and TiCHA+NH_3 periodic models. Distances are given in Å, angles in °, volume in $Å^3$.

Model	**a**	**b**	**c**	**α**	**β**	**γ**	**V**
CHA	16.578	16.582	16.582	111.3	111.4	111.4	3243
Ti-CHA	16.643	16.581	16.639	111.1	111.6	111.5	3263
Ti-CHA+NH_3	16.637	16.611	16.617	111.1	111.6	111.5	3259

In Table S3 the relaxed parameters for the pure siliceous chabazite (CHA), titanium chabazite (TiCHA) and TiCHA+NH_3 adduct single cell models are presented. The introduction of the Ti atom leads to an unrealistic deformation of the crystallographic cell, due to the excessive Ti concentration (Si/Ti = 11).

Table S3. Optimized cell parameters for the CHA, TiCHA and TiCHA+NH_3 single cell periodic models. Distances are given in Å, angles in °, volume in $Å^3$.

Model	**a**	**b**	**c**	**α**	**β**	**γ**	**V**
CHA	9.351	9.351	9.351	94.2	94.2	94.2	811
Ti-CHA	9.536	9.371	9.421	93.6	94.9	93.6	835
Ti-CHA + NH_3	9.542	9.332	9.401	93.4	94.6	93.2	831

In Figure S1 the Complete Basis Set (CBS) BE^c extrapolation for the F9 cluster model is reported. The CBS values were extrapolated keeping constant the cations basis set (Si,Ti: TZVP; H: 6-311++G(2d,2p)), while three different aug-cc-pVnZ basis sets (with n=D,T,Q) were applied to oxygen and nitrogen. The calculated numerical values are given in Table S4. The values obtained with the aug-cc-pVQZ basis are with good approximation matching the CBS extrapolated values, so giving and adequate description of the energetic of the system.

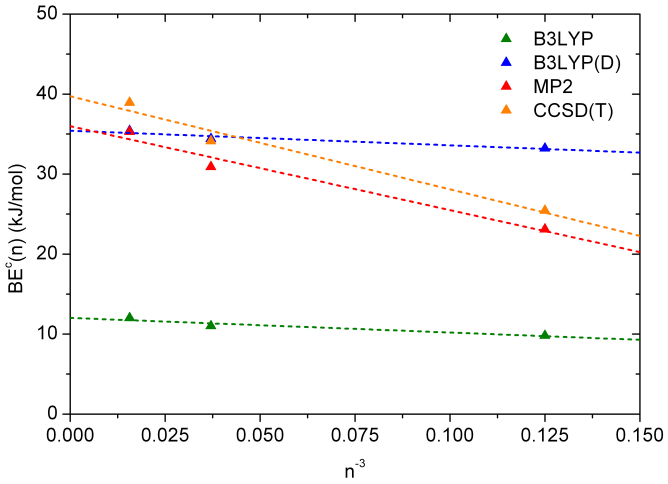

Figure S1. Complete Basis Set extrapolation for the BE^c(HM) of F9 cluster model, where n is the maximum angular momentum of the corresponding aug-cc-pVnZ basis sets.

Table S4. HM BSSE corrected Binding Energies (BE^c(HM)) for the F9 cluster computed with increasing size basis set on O/N atoms. The extrapolated value for the Complete Basis Set (CBS) Binding Energy is reported as well. All the value are reported in kJ/mol.

Method	**aug-cc-pVDZ**	**aug-cc-pVTZ**	**aug-cc-pVQZ**	**CBS**
B3LYP	9.8	11.0	12.0	12.1
B3LYP(D)	33.2	34.4	35.4	35.4
MP2	23.1	30.9	35.3	36.1
CCSD(T)	25.4	34.1	38.9	39.7

In Table S5 the full set of relaxed cell parameters for the CHA, TiCHA and TiCHA+H_2O/NH_3 mono- and bi-adducts periodic models obtained at the B3LYP(D) level are reported.

Table S5. Optimized B3LYP(D) cell parameters for the CHA, TiCHA and TiCHA+H_2O/NH_3 mono- and bi-adducts periodic models. Distances are given in Å, angles in °, volume in $Å^3$.

Model	**a**	**b**	**c**	**α**	**β**	**γ**	**V**
CHA	16.552	16.492	16.491	112.3	111.1	111.1	3180
Ti-CHA	16.622	16.494	16.556	111.9	111.4	111.2	3204
Ti-CHA + H_2O^1	16.612	16.502	16.566	111.9	111.3	111.2	3208
+ H_2O^2	16.658	16.461	16.645	111.2	111.6	112.1	3201
Ti-CHA + NH_3^1	16.628	16.519	16.541	112.0	111.3	111.3	3202
+ NH_3^2	16.713	16.417	16.607	111.8	111.8	111.5	3183